Available online at www.sciencedirect.com

ScienceDirect

Transportation Research Procedia 70 (2023) 284–291

Transportation Research Procedia

www.elsevier.com/locate/procedia

8th International Electric Vehicle Conference (EVC 2023)

Analysis of Electric Vehicles Battery Ageing Associated to Smart Charging Controls

Jorge Nájera[a,*], Jaime R. Arribas[b], Rosa M. de Castro[b], Hugo Mendonça[b], Marcos Blanco[a], Gustavo Navarro[a], Marcos Lafoz[a]

[a]*CIEMAT, Centro de Investigaciones Energéticas, Medioambientales y Tecnológicas, 28040 Madrid, Spain*
[b]*E.T.S.I. Industriales, Universidad Politécnica de Madrid, 28006 Madrid, Spain*

Abstract

EVs smart charging controls emerge as a possibility to overcome voltage quality issues caused by the increasing penetration of EVs in LV networks. However, solving voltage issues implies that EV chargers must deal with reactive power provision, inducing an extra AC ripple in the battery that influences the EV battery lifespan. Four decentralized smart charging controls have been analyzed, modelled and implemented together with a commercial EV charger model and EV battery model that includes both runtime and ageing behavior. Results show that solving voltage issues with EV smart charging controls can lead to a temperature increment in the battery that influences the EV battery lifespan. Nevertheless, this situation can be effectively overcome by minor modifications in the EV charger or in the EV battery cooling system.

Keywords: battery ageing; smart charging; voltage unbalance; under-voltage; LV network.

1. Introduction

The increasing penetration of EVs in low-voltage (LV) distribution networks is likely to become a challenge for distribution system operators (DSOs) since it can lead to power quality issues. The coordinate effect of both EVs and household loads highly contributes to the unbalanced operation of the network, which results in voltage quality concerns such as under-voltage conditions and voltage unbalance.

* Corresponding author. Tel.: +34-91-335-7194.
E-mail address: Jorge.Najera@ciemat.es / Jorge.Najera@externos.ciemat.es

10.1016/j.trpro.2023.11.031

In this framework, EVs smart charging controls emerge as a possibility to overcome those voltage quality issues. Among the specialized literature, smart charging controls can be divided into centralized and decentralized architectures, whose advantages and disadvantages have been discussed in Farooq et al., 2019. Considering that cost and robustness are similar in both architectures, the decentralized control tends to be a more practical solution, since it is based on local measurements and does not need additional communication infrastructure. In addition to the classification between centralized and decentralized architectures, EV smart charging controls can be divided into those controls suitable for being implemented in a single-phase charger, and those applicable to three-phase chargers.

Commonly, the implementation of EV smart charging controls has been studied from the LV network or EV charger operation point of view, using them for reactive power compensation or STATCOM (Nikkhah Mojdehi & Ghosh, 2016 and Zaidi, Sunderland, & Conlon, 2019). Less attention has been paid to the battery given that, theoretically, this reactive power flow does not influence the battery cycling current. However, this extra reactive power that flows through the EV charger induces an extra AC ripple in the battery current, which in turn increases the battery ageing associated to those smart charging controls. This paper analyses the EV battery ageing associated to the implementation of the most relevant decentralized smart charging controls for improving voltage quality in LV networks.

2. EV battery model

In order to analyze the ageing induced in a battery, an EV battery model is needed. The EV li-ion battery model used in this work is the one developed by the authors in Nájera Álvarez, 2020. A brief description of the main components of the model is included in this section, and further information can be found in Nájera Álvarez, 2020. The complete model is an equivalent circuit model which includes three sub-models: voltage/runtime model, thermal model, and ageing model.

2.1. Voltage / runtime model

The voltage/runtime model is based on the Shepherd model which describes the electrochemical behavior in terms of voltage, current, internal resistance and SoC (Moreno-Torres Concha, 2016). The main modification is the representation of the internal resistance, which is modelled as two different electrical resistances, ohmic and polarization, the latter being dependent on the SoC. Since ohmic resistance is almost constant over 20% to 100% SoC, its SoC dependency has not been considered. The model behaves as follows:

$$
\begin{aligned}
E &= f(SoC) = E_0 - K \cdot Q_{MAX}\left(\frac{100}{SoC} - 1\right) + A \cdot e^{-B \cdot Q_{MAX}\left(1 - \frac{SoC}{100}\right)} \\
R_{POL,discharge} &= f(SoC) = K \cdot \frac{100}{SoC} \\
R_{POL,charge} &= f(SoC) = K \cdot \frac{1}{1.1 - \frac{SoC}{100}}
\end{aligned}
\tag{1}
$$

where E is the battery open-circuit voltage [V], SoC is the battery state of charge [%], E_0 is the open-circuit constant voltage, K is the polarization resistance constant [Ω], Q_{MAX} is the battery maximum capacity [Ah], A is the exponential voltage [V], B is the exponential capacity [Ah^{-1}], and R_{POL} is the polarization resistance.

The voltage/runtime model considers the following assumptions: the parameters do not vary for charging and discharging, the Peukert effect and memory effect are negligible, and the ohmic internal resistance is constant.

2.2. Thermal model

Considering temperature-dependent parameters implies modelling the thermal dynamics of the battery. The thermal model implemented is comprised of two parts: a heat generation model and a heat evacuation model. The first one was developed based on the work presented in Saw, Somasundaram, Ye, & Tay, 2014, where three heat sources or mechanisms are considered: irreversible heat (or reaction heat), reversible heat, and ohmic heat.

The second part of the thermal model corresponds to the heat evacuation, both within a single cell and for a whole battery pack. As this part highly depends on the specific battery design under analysis (particularly on those aspects regarding the battery pack and its cooling system), the model takes a simplified approach regarding the whole pack. It assumes that both the heat generation and the internal temperature of the cell are constant and uniform.

$$T(s) = \frac{H \cdot R_{OUT} + T_0}{1 + m \cdot c_p \cdot R_{OUT} \cdot s} = \frac{H \cdot R_{OUT} + T_0}{1 + t_{th} \cdot s} \tag{2}$$

where H is the generated heat [W], T is the cell temperature [K], T_0 is the battery reference temperature [K], m is the mass of the cell [kg], cp specific heat capacity of the cell [J kg^{-1} K^{-1}], R_{OUT} is the resistance for convective heat transfer [K/W], t_{th} is the thermal time constant [s], and s is the Laplace variable.

2.3. Ageing model

The ageing model is a semi-empirical model divided into calendar and cycling ageing. It can be formulated as:

$$Q_{loss} = \left(a \cdot T^2 + b \cdot T + c\right) \cdot e^{(d \cdot T + e) \cdot C_{rate}} \cdot Ah + f \cdot e^{g \cdot SoC} \cdot e^{h/T} \cdot t^z \tag{3}$$

where Q_{loss} is the total lost capacity [%], a to f are parameters dependent on the battery chemistry [-], C_{rate} is the charge/discharge rate [-], Ah is the Ah flown through the battery [Ah], t is the time [day], and z is the power law factor [-], which can take values between 0.5 and 1. Detailed explanation, parameterizations and validations can be found in Nájera Álvarez, 2020.

3. Smart charging controls

The selected decentralized smart charging controls for improving voltage quality levels are the following:

3.1. Active power droop control (Droop P)

Droop P control has been mainly investigated for being implemented in single-phase EV chargers. Among the different Droop P controls in the literature, the one proposed in Geth et al., 2012 has been selected for the analysis since it is the most implemented for EVs (García-Villalobos et al., 2014). The charging control takes the EV's phase voltage measurement and calculates the charging power based on the droop P curve shown in Fig. 1.

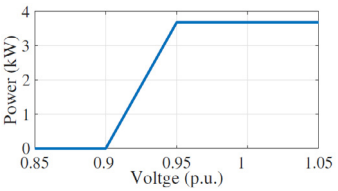

Fig. 1. Droop curve of active power control.

3.2. Reactive power droop control (Droop Q)

The Droop Q control selected for comparison and analysis is the control described in Knezović & Marinelli, 2016. Its main advantage with respect to the Droop P control is that it provides under-voltage and over-voltage regulation without compromising the EV full charge. This control is similar to the Droop P control, but the reactive power is a function of the active power consumed by the EV and the voltage at the EV connection point, $Q = f(P;U)$, as shown in Fig. 2. Unlike the Droop P control, the Droop Q can be bidirectional.

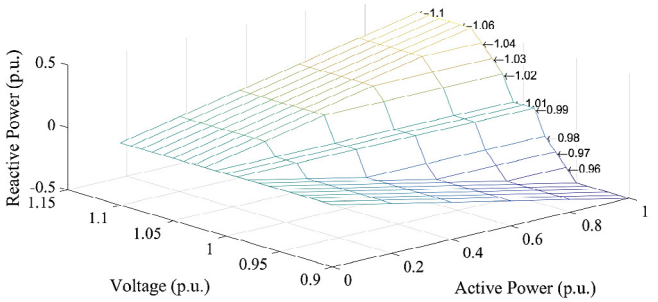

Fig. 2. Droop curve of reactive power control.

3.3. Load balancing control (LB)

The control proposed in Weckx & Driesen, 2015 has been implemented in this paper as a LB control. This charging control is designed for being implemented in a three-phase charger and consists of dividing the EV charging power between the phases based on the phase-to-neutral voltage differences between them. The control behaves as follows:

$$\begin{aligned} P_a &= \frac{P_{EV} + k(U_a - U_b) + k(U_a - U_c)}{3} \\ P_b &= P_a + k(U_a - U_b) \\ P_c &= P_a + k(U_a - U_c) \end{aligned} \tag{4}$$

where P_{EV} is the EV charging power, and k is a parameter that controls the interphase power delivery. For the studies carried out in this work, a constant value of 100 W/V has been selected for this parameter. Besides, the following equations must be accomplished so the power consumed by the EV does not exceed the EV charger maximum power ($P_{EV\,max}$):

$$\begin{aligned} P_{EV} &= P_a + P_b + P_c \\ -P_{EV\,\max} &\le P_a + P_b + P_c \le P_{EV\,\max} \end{aligned} \tag{5}$$

3.4. Sequence compensation control (SC)

The SC control aims for compensating the negative and zero voltage components. The SC control selected is the one proposed in Caldon, Coppo, & Turri, 2014, which is suitable for being implemented in three-phase inverters and behaves as follows:

$$\begin{bmatrix} I_{Ba} \\ I_{Bb} \\ I_{Bc} \end{bmatrix} = \begin{bmatrix} 1 & 1 & 1 \\ 1 & a^2 & a \\ 1 & a & a^2 \end{bmatrix} \begin{bmatrix} -I_{m0} \\ 0 \\ -I_{m2} \end{bmatrix}$$
$$I_{abc} = I_{Babc} + I_{Pabc} \tag{6}$$
$$I_{Pabc} = -\frac{P_{Babc}}{3E_k}$$

where I_{abc} is the three set of compensating currents, and I_{Babc} is the three set of balancing currents that compensate the voltage unbalance originated by the measured currents I_{m0} and I_{m2}.

The balancing currents introduce an undesirable active power that needs to be eliminated by injecting a further balanced set of currents I_{Pabc}. This set equals to the active power originated by I_{Babc} divided by three times the mean value of the phase voltage magnitudes.

4. Battery ageing dependency on the charging control

For the analysis carried out in this work, the four selected controls, whether single-phase or three-phase, charge the EV battery with 3.68 kW. Only Droop P control, which diminishes the charging power according to the voltage level, can vary the EV active power consumption. LB control performs an active power rearrangement between phases to reduce the unbalance, but no reactive power provision is involved in the EV charging process. At last, Droop Q control injects reactive power to the grid for increasing the phase voltage level and SC control balances the current consumed by the EV.

The battery ageing associated to the active power flow through an EV charger has been extensively assessed, but the battery ageing associated to the reactive power flow has barely been analyzed. The main reason for this is that providing reactive power with an EV charger does not have a direct effect on the battery, as an active power flow would. A reactive power provision implies a higher ripple in the battery current, being this ripple function of the charging control, EV charger topology, and DC-link capacitor (Kisacikoglu, Kesler, & Tolbert, 2015 and Kisacikoglu, Ozpineci, & Tolbert, 2011).

Given that this work aims for analyzing the battery ageing associated to charging controls, it is crucial to identify the effects that the current ripple originated by an EV charger has on the battery behavior and ageing. In this sense, authors in Amamra et al., 2020 concluded that high frequency AC ripple has no measurable effect in the internal resistance, and a slight effect is observed in capacity, suggesting that this ripple could contribute to the SEI (solid electrolyte interface) growth. Similar results were obtained in Ghassemi et al., 2021 and Brand et al., 2018, pointing out that a slight capacity loss occur due to the temperature increment experienced by the battery when subjected to high frequency AC ripple. Hence, the battery ageing associated to the four controls can be evaluated with the battery thermal and ageing model described in Section 2.

5. Methodology

In order to study the battery ageing associated to the different controls, a complete EV charger model is needed. The EV charger developed in this work has been modelled in MATLAB Simulink and replicates the bidirectional charger topology located at the ETSII UPM laboratory, described in Nájera Álvarez, 2020. Typical values of commercial EV chargers for the AC inductive filter (1 mH), DC filter (0.3 mH) and for the DC-link capacitor (2.2 mF) have been selected (Kisacikoglu, Ozpineci, & Tolbert, 2011). When performing the simulations, the power grid is considered infinite and the converters as ideal, given that the work developed in this section is not focused on efficiency. Moreover, the low-level control is a standard vector control in dq axis for the inverter that regulates the power exchanged with the grid. The control is modelled based on Yazdani & Iravani, 2010 and Fan, 2017. Moreover, a battery of 355 V and 39 kWh has been selected for the analysis of this section, close to the nominal parameters of

commercial EVs (Nissan, 2010). For parameterizing the battery model, a Kokam NMC cell (Nájera Álvarez, 2020) has been selected, resulting in a configuration of 96s2p.

The model, parameterized as aforementioned, has been tested for different rates of reactive power exchanged with the grid, obtaining the steady state temperature shown in Table 1. A difference of 1.01ºC is observed between 100 VAr and 1000 VAr. The temperature has a linear evolution, which can be adjusted via a least squares method, as shown in Fig. 3.

Table 1. Temperature increment in the battery as a function of the reactive power.

Q [VAr]	100	200	300	400	500	600	700	800	900	1000
T [ºC]	23.58	25.48	25.55	25.66	25.77	25.89	26.02	26.14	26.26	26.39

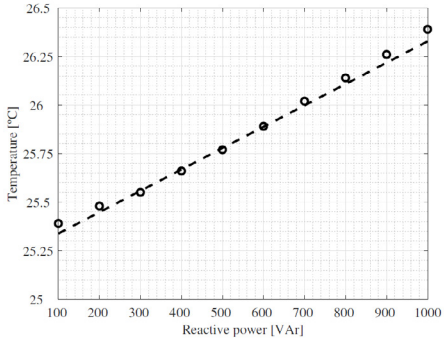

Fig. 3. Temperature increment in the battery as a function of the reactive power.

The controls are compared to a base case charging/discharging scenario. This base case includes one cycle per day, starting with a 100% discharge cycle at 0.1C, and followed by a complete charge with 3.68 kW. The ambient temperature is fixed at 25ºC, and no forced refrigeration is included. The results are evaluated after 1000 complete cycles. A relative comparison between charging controls is proposed, so general trends can be observed. Typical profiles for Droop P, Droop Q and SC controls are selected. LB control is expected to give a result similar to the base case, given that the battery is charging with the same power and no reactive power is involved. The selected profiles are shown in Fig. 4 and Fig. 5, being the former the active power profile for Droop P, and the latter the reactive power profile associated to three Droop Q scenarios: maximum reactive provision, medium reactive provision, and low reactive provision. An SC control typical profile is also included in Fig. 5.

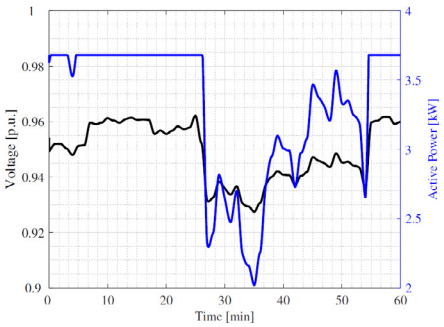

Fig. 4. Typical active power charging profile for Droop P control.

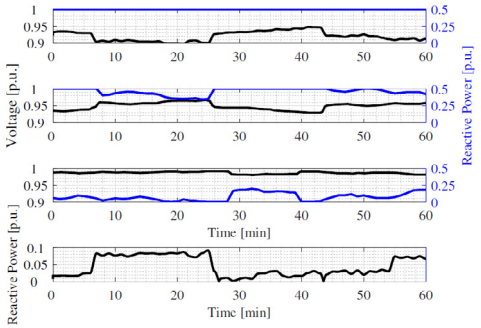

Fig. 5. Typical reactive power profile for Droop Q control (max, med, min), and for SC control.

6. Results

The battery ageing results associated to the different charging profiles are shown in Fig. 6. LB control is not included since there is no appreciable difference with respect to the base case. As expected, little variation is observed between the ageing associated to the maximum and minimum ageing scenarios. A maximum difference of 0.8035% SoH is observed after 1000 cycles between Droop P and Droop Q max scenarios. The best charging control from the battery point of view is Droop P control, since the C rate and temperature variations are diminished with respect to the base case, even though the charging process last longer that in the rest of scenarios. Droop Q scenario experience the highest battery ageing for Droop Q max and Droop Q med, while a slight ageing increment with respect to the base case is observed for Droop Q min and SC control.

As derived from the previous results, dealing with reactive power when improving voltage quality implies an extra AC ripple in the battery cycling current. The amplitude and frequency of this ripple depends on the EV charger topology and control. This ripple can, as shown in Table 1, increase the battery temperature, which in consequence induces a higher ageing in the battery.

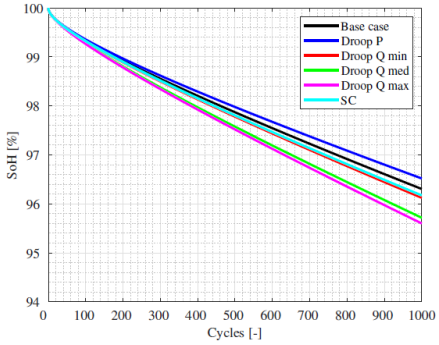

Fig. 6. Battery ageing associated to the different charging profiles.

7. Conclusion

The paper analyzes the battery ageing associated to different EV charging profiles. Providing services further than charging the EV battery can lead to an accelerated ageing, in terms of capacity loss. If those extra services include active power flown through the battery, it is clear that an extra cycling will be induced. However, this is not clear when the EV charger is dealing with reactive power.

The approach taken in this work to evaluate the battery ageing associated to each charging control shows that there are little variations when compared to a base case where the EV charger charges the battery with constant power.

Those variations, which occur due to a higher temperature when dealing with high rates of reactive power, can be effectively solved with a simple cooling system, which is equipped in the majority of EVs. Nevertheless, other simple and straightforward solutions could be taken, such as increasing the size of the DC-link capacitor and, thus, reducing the high frequency AC ripple. According to this, performing voltage issues mitigation with EVs is not limited by the battery lifespan, and could contribute to a better power quality without incurring in a higher battery ageing or a worsened battery behavior.

Acknowledgements

This paper has been partially funded by the research projects "DESARROLLO DE UNA METODOLOGÍA PARA DETERMINAR ARQUITECTURA ÓPTIMA DE SISTEMA HÍBRIDO BASADO EN CONFIGURACIONES DE PILA DE COMBUSTIBLE (MULTYSTACK-HD). Plan nacional. Reference: PID2021-125592OB-I00" and "SEGVAUTO 4.0-CM: SEGURIDAD DE VEHICULOS PARA UNA MOVILIDAD INTELIGENTE, SOSTENIBLE, SEGURA E INTEGRADORA. CONVOCATORIA DE PROGRAMAS DE I+D EN TECNOLOGÍA/2018. Orden 4411/2018, de 13 de diciembre. Reference: S2018/EMT- 4362".

References

Amamra, S.-A., Tripathy, Y., Barai, A., Moore, A. D., & Marco, J. (2020). Electric Vehicle Battery Performance Investigation based on real world current harmonics. *Energies*, *13*(2), 489.

Brand, M. J., Hofmann, M. H., Schuster, S. S., Keil, P., & Jossen, A. (2018). The influence of current ripples on the lifetime of lithium-ion batteries. *IEEE Transactions on Vehicular Technology*, *67*(11), 10438–10445.

Caldon, R., Coppo, M., & Turri, R. (2014). Distributed Voltage Control Strategy for LV networks with inverter-interfaced generators. *Electric Power Systems Research*, *107*, 85–92.

Fan, L. (2017). *Control and dynamics in power systems and microgrids*. CRC Press.

Farooq, S. M., Hussain, S. M., Kiran, S., & Ustun, T. S. (2019). Certificate based security mechanisms in vehicular ad-hoc networks based on IEC 61850 and IEEE Wave Standards. *Electronics*, *8*(1), 96.

García-Villalobos, J., Zamora, I., San Martín, J. I., Asensio, F. J., & Aperribay, V. (2014). Plug-in electric vehicles in Electric Distribution Networks: A review of smart charging approaches. *Renewable and Sustainable Energy Reviews*, *38*, 717–731.

Geth, F., Leemput, N., Van Roy, J., Buscher, J., Ponnette, R., & Driesen, J. (2012). Voltage Droop charging of electric vehicles in a residential distribution feeder. *2012 3rd IEEE PES Innovative Smart Grid Technologies Europe (ISGT Europe)*.

Ghassemi, A., Chakraborty Banerjee, P., Hollenkamp, A. F., Zhang, Z., & Bahrani, B. (2021). Effects of alternating current on Li-ion battery performance: Monitoring degradative processes with in-situ characterization techniques. *Applied Energy*, *284*, 116192.

Kisacikoglu, M. C., Kesler, M., & Tolbert, L. M. (2015). Single-phase on-board bidirectional PEV Charger for V2G Reactive Power Operation. *IEEE Transactions on Smart Grid*, *6*(2), 767–775.

Kisacikoglu, M. C., Ozpineci, B., & Tolbert, L. M. (2011). Reactive Power Operation Analysis of a single-phase EV/PHEV bidirectional battery charger. *8th International Conference on Power Electronics - ECCE Asia*.

Knezović, K., & Marinelli, M. (2016). Phase-wise enhanced voltage support from electric vehicles in a Danish low-voltage distribution grid. *Electric Power Systems Research*, *140*, 274–283.

Moreno-Torres Concha, P. (2016). *Analysis and Design Considerations of an Electric Vehicle Powertrain regarding Energy Efficiency and Magnetic Field Exposure* (Doctoral dissertation, Industriales).

Nájera Álvarez, J. (2020). *Study and Analysis of the Behavior of LFP and NMC Electric Vehicle Batteries concerning their Ageing and their Integration into the Power Grid* (Doctoral dissertation, Industriales).

Nikkhah Mojdehi, M., & Ghosh, P. (2016). An on-demand compensation function for an EV as a reactive power service provider. *IEEE Transactions on Vehicular Technology*, *65*(6), 4572–4583.

Nissan, L. E. A. F. (2010). Nissan leaf.

Saw, L. H., Somasundaram, K., Ye, Y., & Tay, A. A. O. (2014). Electro-thermal analysis of lithium iron phosphate battery for electric vehicles. *Journal of Power Sources*, *249*, 231–238.

Weckx, S., & Driesen, J. (2015). Load balancing with EV Chargers and PV inverters in unbalanced distribution grids. *IEEE Transactions on Sustainable Energy*, *6*(2), 635–643.

Yazdani, A., & Iravani, R. (2010). *Voltage-sourced converters in power systems: modeling, control, and applications*. John Wiley & Sons.

Zaidi, A. H., Sunderland, K., & Conlon, M. (2019). Role of reactive power (STATCOM) in the planning of distribution network with higher EV charging level. *IET Generation, Transmission & Distribution*, *13*(7), 951–959.